ISSN 0361-5219, Solid Fuel Chemistry, 2022, Vol. 56, Suppl. 1, pp. S74–S82. © Allerton Press, Inc., 2022.

Estimation of Biomass Fuels' HHVs Based on Ultimate and Proximate Analysis and Their Combination Data Using MLP-ANN Models

Sevilay Demirci[a,*], Vedat Adiguzel[a,], Muhammet Ali Karabulut[b,***], and Fikret Akdeniz[c,****]**

[a] *Department of Chemical Engineering, Kafkas University, Kars, Turkey*

[b] *Department of Electrical and Electronics Engineering, Kafkas University, Kars, Turkey*

[c] *Department of Chemistry, Kafkas University, Kars, Turkey*

**e-mail: incesevilay@gmail.com*

***e-mail: vedatnursen@gmail.com*

****e-mail: karabulutmali@gmail.com*

*****e-mail: drakdeniz@gmail.com*

Received October 12, 2022; revised October 25, 2022; accepted November 2, 2022

Abstract—The most important thing to know when investigating the feasibility of energy generation from biomass materials is the higher heating values (HHVs). 12 biochars were obtained from zeyrek pulp by hydrothermal carbonization method. Fuel properties (proximate, ultimate and calorific value) and structural properties (by IR spectroscopy) of the obtained biochars were determined. To predict HHVs of biomass, the multi-layer perceptron artificial neural network (MLP-ANN) technique is used. For this purpose, 66 real data points were extracted from both our data and reliable references for the model's training and validation. Based on input data from the proximate analysis, ultimate analysis and combined proximate-ultimate analysis, three different MLP-ANN models were developed. The prediction accuracies of these models were compared statistically to the experimental data. MLP-ANN models have been shown to predict the HHV of biomass with high accuracy. The performance of the MLP-ANN models was also evaluated and it was discovered that the combined proximate-ultimate analysis based MLP-ANN model providing the best results such as coefficient of correlation (R^2), root mean square error (*RMSE*) and mean absolute percentage error (*MAPE*).

Keywords: Higher heating value, Biomass fuels, Proximate analysis, Ultimate analysis, MLP-ANN

DOI: 10.3103/S0361521923010123

1. INTRODUCTION

World energy demand increases in parallel with the increasing population especially in developing economies. Fossil fuels are the most important source in meeting this energy need today. Therefore, due to the environmental pollution of fossil fuels, the possible causes of global warming and the ever-decreasing amount of reserves, many nations have sought new and renewable energy sources [1]. Biomass is one of the most important of them. Biomass is not in a standard composition because it contains a wide variety of animal and vegetable wastes. Its chemical composition, physical properties and thermal properties vary considerably and it is important to determine these properties.

Biomass can be used directly for fuel purposes, or it can be converted into valuable products such as biofuel (biogas, biochar and biodiesel) by performing some thermal processes. Liquefaction, combustion, gasification, carbonization and pyrolysis can be counted among the thermochemical conversion techniques applied for this purpose [1]. Among them, pyrolysis has attracted great interest in recent years as it creates more efficiency and less pollution. Pyrolysis refers to the process of decomposition of biomass in an inert atmosphere at high temperatures to obtain solid, liquid or gaseous products [2, 3].

Biochar is one of the important products obtained from the pyrolysis of biomass; It has the opportunity to be used in many areas such as water and soil treatment processes [4], catalyst for the gasification process [5, 6] and activated carbon production [7]. In addition, due to its high absorbency, biochar is also used in different areas such as improving soil and water quality and controlling erosion [8, 9].

The thermal energy content of biochar is determined by measuring the higher heating value (HHV). HHV measurement is mostly done using the bomb calorimeter. However, this process is often not feasible because experimental equipment is expensive and

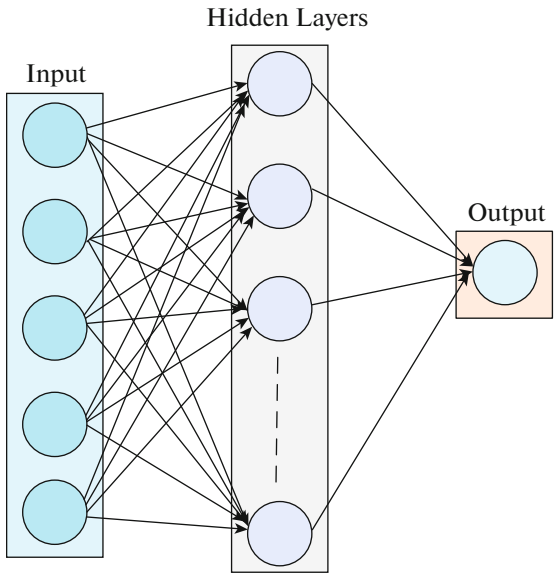

Fig. 1. Schematic diagram of three layer neural network.

requires expertise to use [10, 11]. Therefore, in recent years, a number of studies to create theoretical equations based on some analysis results of biomass HHVs, including proximate analysis, ultimate analysis and structural component analysis that can be obtained with simple and basic equipment [12, 13]. Such equations developed for the estimation of HHVs of biomass are mostly made using proximate and ultimate analysis data [14].

When there is a significant variation in biomass characteristics or HHV depends nonlinearly on input parameters, the correlation base models fail to predict HHV well. As a result, an artificial neural network (ANN) has recently emerged as an advanced tool for predicting the HHV of fuels. ANN models have been used successfully in a variety of fields of study, including engineering, mathematics, medicine, economics and neurology [15]. ANN outperforms correlation-based models in several ways. It can handle large amounts of data, detect complex nonlinear relationships between dependent and independent variables and it can detect all possible interactions between predictor variables. The primary benefit of using ANN models is that it allows users to recognize complex interactions between input and output without requiring a deeper understanding of the underlying scientific process. As a result, many researchers have recently used the ANN model to predict the HHV of biomass [15–19].

Biomass energy resources in Turkey are 135 Mtoe and it is estimated that 65 Mtoe of this can be used. Biomass energy constitutes approximately 13% of the total energy use in Turkey. In general, peanuts, hazelnuts, walnuts, olives, cotton, sesame, sunflower, flaxseed wastes, etc. are sources of biomass in Turkey [2].

In this study, defatted linseed (*Linum usitatissimum* L.) pulp, locally known as zeyrek, grown in the Northeast region of Turkey, was used as biomass. Biochars were obtained from this biomass by hydrothermal pyrolysis method. Numerical formulas are created by using multi-layer perceptron artificial neural network (MLP-ANN) from proximate, ultimate analysis and combination of proximate and ultimate analysis data of the biochars and biomass samples selected from the literature.

2. EXPERIMENTAL

2.1. Hydrothermal Pyrolysis Process

The zeyrek pulp sample used as biomass was dried in an oven at 60°C for 24 hours and then ground in a laboratory-type mill (IKA A11). The biomass sample was separated into various particle sizes with the help of a Retsch AS 200 vibrating sieve (15-20 minutes sieving time at 60 Hz intensity). Samples with a particle size of 125-250 μm were used in the biochar production experiments. Hydrothermal carbonization experiments were carried out in a 200 mL autoclave at a 1 : 4 weight biomass-water ratio at temperatures of 175, 200, 250 and 275°C and at different duration times (10, 30 and 60 minutes) [3, 20]. The biomass-water mixture was placed in the reactor and then the reactor contents were heated to the desired reaction temperature with a heating rate of 5°C/min and kept at this temperature for the desired time. At the end of the process, the reactor was rapidly cooled down to room temperature. The valve was opened and the gases were released into the atmosphere, then the solid residue (biochar) in the reactor was filtered and washed with pure water, then dried in an oven at 105°C. A total of 12 biochar samples were obtained.

Fuel properties (proximate, ultimate and gross calorific value) and structural properties (by IR spectroscopy) of the obtained biochars were determined.

2.2. Biochar Analysis

Proximate, ultimate and higher heating value (HHV) analyses of biochar samples were performed. Proximate analyzes of the samples (ash, moisture, volatile matter and fixed carbon) were performed according to ASTM D1102-84, ASTM D2016-74, ASTM E897-82 and ASTM E870-82 standards, respectively. Ultimate analyzes of the samples (carbon, hydrogen, oxygen, nitrogen and sulfur content) were determined using an Elementar Unicube elemental analyzer. The HHVs of the samples were determined according to the DIN 51900-2 standard using a calorimeter device (IKA C 2000). To determine how the carbonization process changes with temperature and reaction time, total organic carbon yields (TOC) were measured using a TOC-L instrument (Shimadzu). The functional groups in the chemical structures of Zeyrek and

Table 1. Data set for MLP

No.	Ref.	Ultimate Analysis					Proximate Analysis			Measured HHV MJ/kg
		Nitrogen	Carbon	Hydrogen	Sulfur	Oxygen*	FC	VM	ASH	
1	PS	5.3694	58.5046	7.1232	0	29.0028	80.3	17.03	2.67	26.6440
2	PS	4.9683	56.6421	6.6627	0	31.7269	75.93	19.99	4.08	25.0970
3	PS	4.8905	58.1733	6.6319	0	30.3043	77.1	19.17	3.73	25.8880
4	PS	6.0088	57.86	6.4323	0	29.6989	70.28	25.86	3.86	24.9700
5	PS	5.7907	59.9117	6.3421	0	27.9555	67.28	28.07	4.65	26.1170
6	PS	5.9613	60.5102	6.3478	0	27.1807	65.86	29.54	4.6	26.2470
7	PS	6.288	60.7979	5.9664	0	26.9477	57.86	33.77	8.37	26.4330
8	PS	5.1033	66.4738	7.2793	0	21.1436	64.85	29.6	5.55	30.6890
9	PS	5.3592	67.1196	7.3886	0	20.1326	66.03	27.12	6.85	30.6970
10	PS	5.1652	65.3258	6.1493	0	23.3597	56.89	35.77	7.34	29.1410
11	PS	5.3095	67.2987	7.5555	0	19.8363	65.82	26.77	7.41	31.0640
12	PS	5.6776	70.1472	7.3743	0	16.8009	62.39	31.79	5.82	32.0070
13	PS	4.9046	48.771	6.5457	0	39.7787	79.19	15.51	5.3	20.7130
14	[23]	0.55	83.67	3.56	1.05	11.17	94.59	7.09	8.32	32.8560
15	[24]	0.57	63.89	4.97	0.48	30.09	49.03	49.47	4.5	25.1000
16	[12]	0.95	46.9	6.07	0	46.08	14.59	83.32	2.09	18.2610
17	[25]	0.48	49.14	6.34	0.02	44.02	19.8	79.1	1.1	19.4230
18	[26]	0.08	48.1	5.99	0	45.83	23.5	76.4	0.1	19.9160
19	[12]	0.03	48.15	5.87	0	45.95	18.52	81.02	1.2	19.7770
20	[27]	0.66	51.3	5.29	0.01	42.74	21.54	76.83	1.63	20.0100
21	[28]	1.8	45.5	5.1	0	47.6	23.5	63	13.5	17.0000
22	[27]	1.2	39.47	5.07	0.02	54.24	17.3	65.4	17.3	15.8300
23	[27]	0.45	50.29	5.05	0.16	44.05	29.7	66.58	3.72	20.0500
24	[29]	0	48.12	6.55	0	45.33	28.06	62.54	9.4	20.6000
25	[28]	0.5	48.6	5.5	0	45.4	13.6	85	1.4	17.1000
26	[25]	0.06	48.67	6.03	0.04	45.2	9.2	90.6	0.2	18.9340
27	[30]	0.2	75.6	3.3	0.2	20.7	67.7	30	2.3	28.8440
28	[30]	0.4	67.7	2.4	0.2	29.3	59.3	25.8	14.9	24.7960
29	[12]	1.38	88.95	0.73	0	8.94	87.17	9.93	2.9	31.1240
30	[31]	0.4	92.7	1.6	0	5.3	91.5	6.6	1.9	32.2040
31	[32]	0.53	92.04	2.45	1	3.98	89.1	9.88	1.02	34.3880
32	[27]	0.36	54.41	4.99	0.01	40.23	23.68	75.92	0.4	21.0100
33	[27]	0.56	48.79	5.91	0.01	44.73	16.84	82.03	1.13	19.2600
34	[33]	5.95	37.23	5.34	0	51.48	11.8	70.1	18.1	15.5300
35	[27]	0.47	46.58	5.87	0.01	47.07	18.54	80.1	1.36	18.7700
36	[28]	0.4	49	5.4	0	45.2	12.5	86.5	1	17.0000
37	[25]	0.08	48.1	5.99	0	45.83	23.5	76.4	0.1	19.9160
38	[27]	0.07	47.84	5.8	0.01	46.28	11.3	88.2	0.5	18.9810
39	[28]	0.05	50.64	5.98	0.03	43.3	19.92	79.72	0.36	20.7200
40	[31]	0.2	52.01	6.1	0	41.69	28.1	70	1.7	20.0000
41	[12]	0.1	47.3	6	0	46.6	17.9	82	0.1	20.0800
42	[27]	0.3	46.04	5.82	0	47.84	21.3	75.35	3.35	18.6400
43	[34]	0.15	48.33	5.89	0.01	45.62	16.93	82.55	0.52	19.3500

Table 1. (Contd.)

No.	Ref.	Ultimate Analysis					Proximate Analysis			Measured HHV MJ/kg
		Nitrogen	Carbon	Hydrogen	Sulfur	Oxygen*	FC	VM	ASH	
44	[27]	0	56.2	5.9	0	37.9	25.8	73	1.2	22.9800
45	[33]	0.83	46.59	5.85	0.04	46.69	19.2	78.63	2.17	19.0300
46	[33]	1.61	48.2	6.25	0	43.94	20.8	78.5	0.7	19.9670
47	[27]	0.17	35.97	5.28	0	58.58	11.8	72.7	15.5	14.5220
48	[33]	0.05	49	5.98	0.01	44.96	16.58	83.17	0.25	19.9500
49	[33]	2.02	49.37	6.4	0	42.21	16.2	83.6	0.2	18.5020
50	[33]	1.33	47.67	6.13	0	44.87	21.8	76.5	1.7	19.8420
51	[33]	0.17	39.75	5.55	0	54.53	14.9	77.4	7.7	17.4100
52	[33]	4.29	36.2	4.72	0	54.79	22.5	57.2	17.3	18.1250
53	[16]	0.51	44.23	6.61	0	48.65	22.8	75.1	2.1	18.3560
54	[16]	0	44.65	6.765	0.235	48.35	4.85	67.95	16.2	18.3600
55	[16]	0	45.28	6.908	0.256	47.556	8.16	64.73	14.71	19.9700
56	[16]	0	43.78	6.652	0.145	49.423	2.81	69.62	17.63	17.1300
57	[16]	0	43.58	6.586	0.237	49.577	13.2	66.97	9.83	19.1600
58	[16]	0	43.56	5.631	0.825	49.984	3.28	70.37	16.35	17.5100
59	[16]	2.3	61	8.5	0	28.2	10.7	77	5.6	28.0500
60	[35]	0.28	45.11	5.91	0.19	48.51	13.04	80.4	5.52	19.8000
61	[35]	0.57	47.69	5.7	0.04	46	9.08	88.04	2.51	20.1000
62	[35]	0.2	50	6	0.01	43.79	15.89	82.92	0.9	21.8000
63	[35]	0.51	47.9	6.1	0.19	45.3	16.19	79.87	3.5	18.1100
64	[35]	0.22	48.9	5.38	0.02	45.03	22.8	73.7	3.2	19.9800
65	[35]	0.45	47.31	6.15	0.1	45.99	14.88	83.82	1.3	18.6000
66	[35]	1.75	41.12	5.29	0.06	51.68	23.95	66.87	9.88	17.2300

* The amount of oxygen was found by subtracting the total difference, PS: Presented study.

biochars were determined using a IR spectrophotometer (Perkin Elmer Frontier FT).

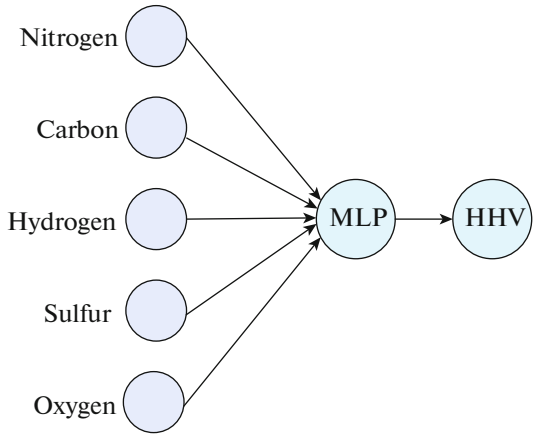

Fig. 2. A brief summary of the current study.

Proximate, ultimate and higher heating value (HHV) measurements were repeated at least three times to ensure the accuracy of the experimental results.

2.3. The multilayer perceptron (MLP)

The multilayer perceptron (MLP) is built on statistical learning theories that are applicable to making a relationship among input variables and are suitable for solving nonlinear problems. In other words, the MLP can connect input and output variables without requiring a complex mathematical and computational methods [21]. Three layer schematic neural network diagram which is consist of input, hidden, and output, is shown in Figure 1.

Our experiments and some related works resulted in a set of 66 data points containing HHVs in terms of nitrogen, carbon, hydrogen and sulfur percentage [1–5]. Figure 2 depicts a summary of the current study.

Table 2. TOC analysis results of biochar samples

Sample*	TOC, %	TC, %	IC, %	Sample*	TOC, %	TC, %	IC, %
175-10	54.76	54.85	0.09512	250-10	55.93	55.98	0.05657
175-30	53.46	53.51	0.04950	250-30	61.28	61.34	0.06050
175-60	55.06	55.11	0.04703	250-60	62.46	62.50	0.03879
200-10	53.36	53.43	0.06724	275-10	60.25	60.33	0.07833
200-30	54.28	54.36	0.07516	275-30	60.91	61.02	0.10960
200-60	55.18	55.22	0.03726	275-60	63.63	63.72	0.09138

TOC: total organic carbon, TC: total carbon, IC: total inorganic carbon * The process–temperature–time sequence was used to name the char samples (e.g., 175-10 stands for hydrothermal carbonization at 175°C for 10 minutes).

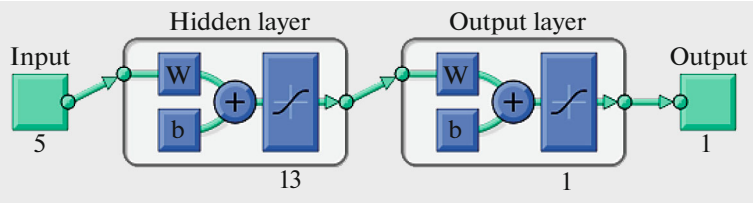

Fig. 3. Structure of MLP-1 for ultimate analysis.

The primary goal of this study is to estimate the HHV of biomass as a target parameter using an MLP algorithm. Various analyses were performed to assess the effectivity of MLP in the estimation of HHVs. The obtained results demonstrated that MLP had a high level of ability and accuracy in predicting the target parameter (HHV of biomass). The root mean square error (RMSE) and mean square error (*MSE*) for each step of the process were also calculated to demonstrate the performance and applicability of this artificial intelligence approach [22]. Based on the findings of this study, it is possible to conclude that MLP could be used as a useful tool in a variety of industrial processes. Table 1 contains a list of 66 of our samples as well as randomly selected samples from the datasets.

3. RESULTS AND DISCUSSION

In this study, the data of 12 biochar samples obtained from zeyrek pulp by the hydrothermal method were used. The structural and fuel properties of the obtained biochars were investigated. By using this biomass and the proximate and ultimate analysis data of the obtained biochars and the analysis data found in the literature, formulas for calculating the most appropriate theoretical HHVs for the experimental HHVs were created. Among the obtained formulas, the most appropriate one was selected and its compatibility with the literature data was investigated.

To determine how the carbonization process changes with temperature and reaction time, the total organic carbon yields of the obtained biochars were measured (Table 2). As can be seen from the table, the amount of TOC increased with the increase in temperature.

According to the IR spectra of raw materials and all biochars, 3216-3299 cm^{-1} –OH, 2922–2856 cm^{-1} aliphatic CH, 1641–1703 cm^{-1} C=O, 1451–1535 cm^{-1} aromatic C=C, C–O–C peaks between 1156–1165 cm^{-1} were found (Figure S1).

3.1. Prediction equation based on ultimate analysis

There are five input parameters in the ANN model based on ultimate analysis: Nitrogen, Carbon, Hydrogen, Sulfur and Oxygen. HHV is the output parameter. An input matrix is made up of five input parameters. The experimental HHV values are used to generate one output matrix. Based on the trial and error method, 13 neurons are considered in the hidden layers for HHV prediction. Figure 3 depicts the MLP-1 structure as determined by ultimate analysis.

Table 3. Comparisons of correlation equations in each scenario

Equation	*R*-Squared	*RMSE*	*MSE*	*MAE*	*MAPE*
MLP-1	0.9929	0.4835	0.2342	0.4687	0.0236
MLP-2	0.9681	0.5331	0.2911	0.5868	0.0257
MLP-3	0.9965	0.4150	0.1724	0.3547	0.0136

Table 4. Comparisons of correlation equations in each scenario

No.	Measured HHV MJ/kg	MLP-1		MLP-2		MLP-3	
		Predicted HHV MJ/kg	Relative Error (%)	Predicted HHV MJ/kg	Relative Error (%)	Predicted HHV MJ/kg	Relative Error (%)
1	26.6440	26.4951	0.5619	29.1669	8.6500	26.5839	0.2262
2	25.0970	25.1905	0.3713	28.4683	11.8422	25.3082	0.8346
3	25.8880	25.7370	0.5868	28.6547	9.6552	25.8573	0.1186
4	24.9700	25.8564	3.4283	27.6129	9.5714	25.6657	2.7106
5	26.1170	26.5010	1.4492	27.1375	3.7604	26.3513	0.8893
6	26.2470	26.8070	2.0889	26.9224	2.5086	26.6075	1.3549
7	26.4330	26.6982	0.9935	25.6154	3.1919	26.5242	0.3438
8	30.6890	29.6789	3.4034	26.7462	14.7414	29.8486	2.8157
9	30.6970	30.1299	1.8823	26.8954	14.1348	30.3738	1.0641
10	29.1410	28.2241	3.2485	25.4919	14.3149	28.2081	3.3074
11	31.0640	30.3331	2.4095	26.8503	15.6935	30.6486	1.3554
12	32.0070	31.4317	1.8302	26.3652	21.3985	31.5072	1.5863
13	20.7130	21.9558	5.6605	28.9361	28.4181	22.1748	6.5923
14	32.8560	32.4153	1.3596	32.9105	0.1657	32.9286	0.2205
15	25.1000	25.3277	0.8989	24.8715	0.9186	25.3918	1.1491
16	18.2610	19.2862	5.3158	19.1729	4.7564	19.1026	4.4055
17	19.4230	20.2566	4.1150	19.9897	2.8349	20.1909	3.8033
18	19.9160	19.3569	2.8883	20.5767	3.2109	19.2980	3.2025
19	19.7770	19.2488	2.7443	19.9182	0.7089	19.2159	2.9198
20	20.0100	20.2138	1.0082	20.2422	1.1473	20.0066	0.0171
21	17.0000	18.1762	6.4710	20.2618	16.0983	18.5393	8.3027
22	15.8300	15.5633	1.7138	19.2282	17.6732	16.1764	2.1417
23	20.0500	19.6689	1.9374	21.4359	6.4653	19.5838	2.3806
24	20.6000	19.8427	3.8168	21.0526	2.1500	20.5628	0.1807
25	17.1000	19.2687	11.2552	19.0384	10.1814	19.0139	10.0656
26	18.9340	19.6507	3.6471	18.3965	2.9220	19.3989	2.3968
27	28.8440	28.0085	2.9831	27.2567	5.8237	28.0656	2.7737
28	24.7960	24.1518	2.6671	25.6812	3.4470	24.7340	0.2506
29	31.1240	31.1878	0.2045	30.2078	3.0329	31.0575	0.2142
30	32.2040	33.0846	2.6617	30.8908	4.2511	33.2703	3.2049
31	34.3880	34.6512	0.7595	30.5460	12.5779	34.1081	0.8205
32	21.0100	21.0543	0.2106	20.5971	2.0048	20.8006	1.0065
33	19.2600	19.7486	2.4740	19.5382	1.4238	19.5679	1.5733
34	15.5300	16.7064	7.0416	18.3718	15.4682	16.5125	5.9500
35	18.7700	18.8065	0.1941	19.7917	5.1622	18.6684	0.5443
36	17.0000	19.2978	11.9071	18.8803	9.9588	19.0043	10.5466
37	19.9160	19.3569	2.8883	20.5767	3.2109	19.2980	3.2025
38	18.9810	19.0882	0.5617	18.7092	1.4525	18.8637	0.6220
39	20.7200	20.3684	1.7261	20.0254	3.4688	20.2662	2.2392
40	20.0000	21.0444	4.9626	21.2057	5.6856	21.1444	5.4122
41	20.0800	19.0581	5.3623	19.7238	1.8058	18.9255	6.1003
42	18.6400	18.4736	0.9007	20.1653	7.5638	18.5301	0.5931
43	19.3500	19.3935	0.2242	19.5662	1.1051	19.2428	0.5569

Table 4. (Contd.)

No.	Measured HHV MJ/kg	MLP-1		MLP-2		MLP-3	
		Predicted HHV MJ/kg	Relative Error (%)	Predicted HHV MJ/kg	Relative Error (%)	Predicted HHV MJ/kg	Relative Error (%)
44	22.9800	22.4395	2.4086	20.9011	9.9462	22.4933	2.1637
45	19.0300	18.9590	0.3743	19.8732	4.2427	18.7922	1.2654
46	19.9670	20.2126	1.2152	20.1514	0.9150	19.9301	0.1850
47	14.5220	13.9626	4.0061	18.4329	21.2169	14.6171	0.6508
48	19.9500	19.7015	1.2614	19.5193	2.2067	19.5627	1.9800
49	18.5020	20.9657	11.7512	19.4626	4.9354	20.5462	9.9492
50	19.8420	19.7885	0.2704	20.2802	2.1607	19.6134	1.1654
51	17.4100	15.6985	10.9023	19.0883	8.7924	15.9292	9.2959
52	18.1250	15.1079	19.9705	19.5102	7.0999	15.0743	20.2374
53	18.3560	18.5563	1.0796	20.4231	10.1213	18.6424	1.5364
54	18.3600	18.9057	2.8862	15.4880	18.5437	19.2237	4.4931
55	19.9700	19.3050	3.4445	15.7891	26.4798	19.5235	2.2868
56	17.1300	18.3694	6.7472	15.3239	11.7865	18.8436	9.0937
57	19.1600	18.3242	4.5610	17.0794	12.1822	18.3328	4.5124
58	17.5100	18.0403	2.9396	15.4153	13.5883	17.7446	1.3223
59	28.0500	27.5645	1.7612	17.3590	61.5876	27.5034	1.9874
60	19.8000	18.3721	7.7722	18.6795	5.9987	18.3017	8.1865
61	20.1000	19.1581	4.9162	18.2609	10.0706	18.8951	6.3765
62	21.8000	20.1709	8.0764	19.3496	12.6638	20.0335	8.8175
63	18.1100	19.7321	8.2207	19.3087	6.2080	19.5859	7.5355
64	19.9800	19.2149	3.9816	20.3462	1.8000	19.2216	3.9454
65	18.6000	19.4315	4.2791	19.2357	3.3047	19.2268	3.2602
66	17.2300	16.6676	3.3740	20.5344	16.0920	16.8179	2.4503
		Average:	3.6213	Average:	8.8863	Average:	3.3740

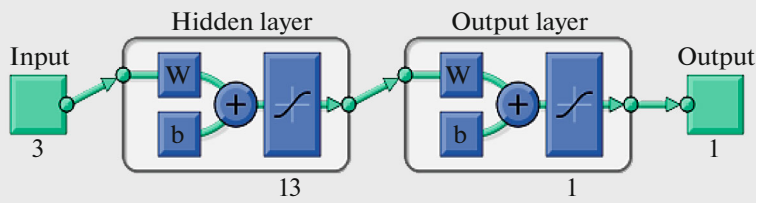

Fig. 4. Structure of MLP-2 for proximate analysis.

3.2. Prediction equation based on proximate analysis

In the case of the ANN model based on proximate analysis, three input parameters are used: FC, VM and ASH. The output parameter is HHV. An input matrix is formed by arranging three input parameters. From the experimental HHV values, one output matrix is created. Based on the trial and error method, 13 neurons are considered in the hidden layers for predicting the HHV. Figure 4 depicts the MLP-2 structure for the proximate analysis.

3.3. Prediction equation based on the combination of proximate and ultimate analysis

The ANN model based on combined proximate and ultimate analysis uses eight input parameters: N, C, H, S, O, FC, VM and ASH. An input matrix is made up of eight input parameters. The experimental HHV values are used to generate one output matrix. Based on the trial and error method, 13 neurons are considered in the hidden layers of this ANN structure.

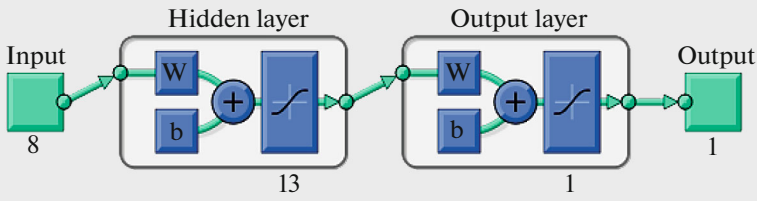

Fig. 5. Structure of MLP-3 for combined proximate-ultimate analysis.

The MLP-3 structure for combined proximate-ultimate analysis is depicted in Figure 5.

3.4. Validation of the correlation equations

A large dataset of proximate and ultimate HHV analyses is compiled from various sources [16]. The database was divided into training (75%) and test (25%) sets for the development of the MLP-based models. Back propagation based Levenberg–Marquardt algorithm was used in the training algorithm. While the training set is used to build the models, the test sets were used to evaluate and validate the models' generalization capability. Each model's performance is evaluated using statistical quantities such as coefficient of correlation (R^2), root mean square error (*RMSE*) and mean absolute percentage error (*MAPE*), as defined below; these are computed using the experimental and model-predicted HHV (MJ/kg) magnitudes.

$$RMSE = \sqrt{\frac{1}{N}\sum_{j=1}^{N}(P_j - C_j)^2}, \quad (1)$$

$$MSE = \frac{1}{N}\sum_{j=1}^{N}(P_j - C_j)^2, \quad (2)$$

$$MAE = \frac{1}{N}\sum_{j=1}^{N}|P_j - C_j|, \quad (3)$$

$$MAPE = \frac{1}{N}\sum_{j=1}^{N}\left|\frac{P_j - C_j}{C_j}\right|, \quad (4)$$

$$R^2 = \frac{N\left(\sum_{j=1}^{N}P_jC_j\right) - \left(\sum_{j=1}^{N}P_j\right)\left(\sum_{j=1}^{N}C_j\right)}{\sqrt{\left(N\sum_{j=1}^{N}(P_j)^2 - (C_j)^2\right)\left(N\sum_{j=1}^{N}(C_j)^2 - (P_j)^2\right)}}, \quad (5)$$

where N denotes the total number of data points, P is the estimated average temperature and C is the average calculated temperature. Table 3 displays the calculated values of R, *RMSE*, *MSE*, *MAE*, and *MAPE* for three MLP-ANN models, which indicate prediction accuracy. The R values for all three MLP-ANN models are reasonably high, indicating that all three MLP-ANN models have very good prediction accuracy. It is also discovered that the MLP-ANN model MLP-3 has the highest R value (0.9965) and the lowest RMSE (0.4150), MSE (0.1724), MAE (0.3547), and MAPE (0.0136) values of the three ANN models. This confirms that the MLP-ANN model based on combined proximate-ultimate analysis can make the most accurate prediction of HHV.

A comparison of HHV prediction accuracy and generalization performance of MLP-based and existing models was performed on the basis of model-predicted and corresponding experimental studies. Parikh's HHV model [12] based on proximate analysis was used for comparison with MLP models of existing models. In the case of models based on ultimate analysis, MLP models are evaluated against the respective models by Channiwala and Parikh, Milne and Friedl [34, 35]. Ozveren U [38]used the ANN model to predict the gross heating value of lignocellulosic fuels and found that it performed better with lower *MAPE* (4.20%) and *RMSE* (0.0460%) than the nonlinear regression model and published correlations. Darvishan et al. [15] used the multilayer perception (MLP) ANN method to predict HHV using proximate analysis data from 78 samples from the published literature. They reported correlation coefficient values of 0.998 and 0.993 for training and testing sets, respectively. Another study predicted HHV from proximate analysis data using the MLP-ANN method, with reported correlation coefficient values of 0.92 for the training step and 0.90 for the testing step [39].

Table 4 compares estimated HHVs from different MLP-ANN models with measured HHVs as well as error performances of each MLP-ANN system. It is seen that the average error percentage for MLP-1, MLP-2 and MLP-3 are 3.6214%, 8.8864% and 3.3741%, respectively. As can be seen from Table 4, it is clear that the best predicted rate is the MLP-3.

4. CONCLUSIONS

In this study, 12 types of biochars with high calorific values were obtained from zeyrek pulp, which has a waste potential. It was observed that HHV increased in parallel with the increase in temperature. Three ANN models based on proximate analysis, ultimate analysis and combined proximate-ultimate analysis of different biomass are developed in this study. It is discovered that the HHVs predicted by all ANN models closely track the experimental HHVs, with a correlation coefficient value greater than 0.964. The devel-

oped ANN model based on the combination of proximate and ultimate analysis outperforms the others, with correlation coefficients, *RMSE*, *MSE*, *MAE* and *MAPE* values of 0.9967, 0.4151, 0.1723, 0.3546 and 0.0138, respectively. The prediction accuracies of these ANN models outside of biomass are assessed by predicting HHVs for another set of biomass samples from the literature. In this study, average error percentage is lower compared to published studies such as [10, 40, 41]. It was revealed that the best prediction performance was obtained from the MLP-ANN 3 model, which is consist of combination of two separate analysis dataset, proximate and ultimate analyses, given in Eq. (3).

ACKNOWLEDGMENTS

The authors would like to acknowledge the Kafkas University for their support under the grant number of 2018-FM-17.

CONFLICT OF INTEREST

The authors declare that there is no conflict of interest with any other research group or institution.

SUPPLEMENTARY INFORMATION

The online version contains supplementary materia available at DOI: 10.3103/S0361521923010123.

REFERENCES

1. Motasemi, F. and Afzal, M.T., *Renew. Sustain. Energy Rev.*, 2013, vol. 28, p. 317.
2. Acikgoz, C. and Kockar, OM., *J. Anal. Appl. Pyrolys.*, 2009, vol. 85, p. 151.
3. Pavkov, I., Radojcin, M., Stamenkovic, Z., Bikic, S., Tomic, M., Bukurov, M., et al., *Solid Fuel Chem.*, 2022, vol. 56, p. 225.
4. Qiu, M., Liu, L., Ling, Q., Cai, Y., Yu, S., Wang, S., et al., *Biochar*, 2022, vol. 4, p. 1.
5. Yang, H., Chen, Z., Chen, W., Chen, Y., Wang, X., and Chen, H., *Energy*, 2020, vol. 210, p. 118646.
6. Yao, D., Hu, Q., Wang, D., Yang, H., Wu, C., Wang, X., et al., *Biores. Technol.*, 2016, vol. 216, p. 159.
7. Rodriguez-Reinoso, F., Molina-Sabio, M., and Gonzalez, M.T., *Carbon*, 1995, vol. 33, p. 15.
8. Mullen, C.A., Boateng, A.A., Goldberg, N.M., Lima, I.M., Laird, D.A., and Hicks, K.B., *Biomass Bioenergy*, 2010, vol.34, p. 67.
9. Cha, J.S., Park, S.H., Jung, S.-C., Ryu, C., Jeon, J.-K., Shin, M.-C., et al., *J. Industr. Eng. Chem.*, 2016, vol. 40, p. 1.
10. Majumder, A.K., Jain, R., Banerjee, P., and Barnwal, J.P., *Fuel*, 2008, vol. 87, p. 3077.
11. Nhuchhen, D.R. and Salam, PA., *Fuel*, 2012, vol.99, p. 55.
12. Parikh, J., Channiwala, S.A., and Ghosal, G.K., *Fuel*, 2005, vol. 84, p. 487.
13. Maksimuk, Y., Antonava, Z., Krouk, V., Korsakova, A., and Kursevich, V., *Fuel*, 2020, vol. 263, p. 116727.
14. Wahid, F.R.A.A., Saleh, S., and Samad, N.A.F.A., *Energy Procedia,* 2017, vol. 138, p. 307.
15. Darvishan, A., Bakhshi, H., Madadkhani, M., Mir, M., and Bemani, A., *Energy Sources, A: Recovery, Utilization, Environmental Effects,* 2018, vol. 40, p. 2960.
16. Pattanayak, S., Loha, C., Hauchhum, L., and Sailo, L., *Biomass Convers. Biorefinery*, 2021, vol. 11, p. 2499.
17. Ozkan, K., Isik, S., Gunkaya, Z., Ozkan, A., and Banar, M.A., *Waste Manage.*, 2019, vol. 100, p. 327.
18. Hosseinpour, S., Aghbashlo, M., and Tabatabaei, M., *Fuel*, 2018, vol. 222, p. 1.
19. Hosseinpour, S., Aghbashlo, M., Tabatabaei, M., and Mehrpooya, M., *Energy*, 2017, vol. 138, p. 473.
20. Pala, M., Kantarli, I.C., Buyukisik, H.B., and Yanik, J., *Biores. Technol.*, 2014, vol. 161, p. 255.
21. Pal, S.K. and Mitra, S., *Multilayer Perception, Fuzzy Sets, Classification*, 1992.
22. Wilamowski, B.M., *Neural Network Architectures and Learning Algorithms, Industrial Electronics Magazine,* 2009.
23. Technology, I., *Preparation of a Coal Conversion Systems Technical Data Book,* Department of Energy, 1976.
24. Bliek, A., *Mathematical Modeling of a Cocurrent Fixed Bed Coal Gasifier*, 1984.
25. Rossi, A., *Progress in Biomass Conversion*, 1984, p. 69.
26. Jenkins, B.M., *Downdraft Gasification Characteristics of Major California Residue-Derived Fuels*, Univ. of California, Davis, 1980,
27. Jenkins, B. and Ebeling, J., *Correlation of Physical and Chemical Properties of Terrestrial Biomass with Conversion: Symp. Energy from Biomass and Waste*, IX IGT, 1985, p. 371.
28. Demirbas, A., *Fuel*, 1997, vol. 76, p. 431.
29. Grover, P.D. and Anuradha, G., *Report on Physico-Chemical Parameters of Biomass Residues*, Delhi: IIT, 1988.
30. Boley, C.C. and Landers, W.S., *Entrainment Drying and Carbonization of Wood Waste*, US Department of the Interior, Bureau of Mines, 1969.
31. Cordero, T., Marquez, F., Rodriguez-Mirasol, J., and Rodriguez, J.J., *Fuel*, 2001, vol. 80, p. 1567.
32. Rose, J.W. and Cooper, J.R., *Technical Data on Fuel, World Energy Conf., London: British National Committee*, 1977, 7th ed.
33. Grover, P.D, Iyer P.V.R, and Rao, T.R., *Biomass: Thermochemical Characterization*, Delhi: MNES, 2002, 3rd ed.
34. Tillman, D.A., *Wood as an Energy Resource*, New York: Academic Press, 1978.
35. Onokwai, A.O., Okokpujie, I.P., Ajisegiri, E.S., Oki, M., Adeoyeb, A.O., and Akinlabi E.T., *Int. J. Renew. Energy Developm.,* vol. 11, p. 973.
36. Channiwala, S.A. and Parikh, P.P., *Fuel*, 2002, vol. 81, p. 1051.
37. Friedl, A., Padouvas, E., Rotter, H., and Varmuza, K., *Anal. Chim. Acta*, 2005, vol. 544, p. 191.
38. Ozveren, U., *J. Energy Inst.*, 2017, vol. 90, p. 397.
39. Keybondorian, E., Zanbouri, H., Bemani, A., and Hamule, T., *Energy Sources, A: Recovery, Utilization, Environmental Effects,* 2017, vol. 39, p. 2105.
40. Tan, Y.L., Abdullah, A.Z., and Hameed, B.H., *Biores. Technol.*, 2017, vol. 243, p. 85.
41. Marx, S., Chiyanzu, I., and Piyo, N., *Biores. Technol.*, 2014, vol. 164, p. 177.